Submitted, 2010 Conference on Decision and Control
http://www.cds.caltech.edu/~murray/papers/lsm10-cdc.html

Synthesis of Embedded Control Systems with High Sampling Frequencies

Javad Lavaei, Somayeh Sojoudi and Richard M. Murray

***Abstract*— Motivated by current technological advances in the design of real-time embedded systems, this work deals with the digital control of a continuous-time linear time-invariant (LTI) system whose output can be sampled at a high frequency. Since a typical sampled-data controller operating at a high sampling frequency needs heavy (high-precision) computation to alleviate its sensitivity to measurement and computational errors, the objective is to design a robust hybrid controller for high-frequency applications with limited computational power. To this end, we exploit our recent results on delay-based controller design and propose a digital-control scheme that can implement every continuous-time stabilizing (LTI) controller. This robust hybrid controller, which consists of an ideal sampler, a digital controller, a number of modified second-order holds and possibly a unity feedback, can operate at arbitrarily high sampling frequencies without requiring expensive, high-precision computation. Later on, it is discussed how to find a continuous-time LTI controller satisfying prescribed design specifications so that its corresponding digital controller requires the least processing time.**

I. Introduction

Since the invention of *digital circuits* and *digital computers* in 1937, there has been an every-growing interest in the digital control of continuous-time systems. Computer controlled systems have been widely used in a broad range of applications from robotics, autopilot and radar to anti-lock braking systems [1], [2]. A typical digital-control scheme for a continuous-time system is composed of an analog-to-digital converter (*sampler*), a digital processor and a digital-to-analog converter (*holder*). This configuration is referred to as *sampled-data control system* and has been long studied in the literature [3], [4], [5].

Among many problems that have been investigated in the context of sampled-data control systems, one can name stability, robustness, sensitivity and frequency-domain characterization. For instance, the paper [6] introduces a lifting technique to design H_2 and H_∞ sampled-data controllers. The work [7] tackles the H_2 sampled-data control problem using a new frequency response operator. The best achievable tracking performance in sampled-data systems are studied in [8]. The works [9] and [10] tackle the stability and tracking capabilities of sampled-data systems with uncertain and time-varying sampling frequencies. Sparked by the pioneering work [11] on multi-rate systems, a linear-matrix-inequality method is proposed in [12] for the robust synthesis of multi-rate sampled-data systems.

Although the works surveyed above consider the hold device to be an ideal zero-order hold, there are other types of holders studied in the literature. A generalized sampled-data hold function (GSHF) is a common substitute for a zero-order hold [13], [14]. The early work [15] shows that a GSHF acts as a state feedback controller without requiring a state estimator. Furthermore, it is known that GSHFs are very effective in simultaneous stabilization [16] and decentralized stabilization of systems with unstable decentralized fixed modes [17].

The current silicon technology has enabled the design of embedded systems operating at very high frequencies [18]. However, the conventional methods for the synthesis of sampled-data control systems require high processing power to cope with numerical issues if the sampling rate is relatively fast. More precisely, increasing the sampling frequency makes the digital controller extremely sensitive to measurement noise and computational round-off errors. Based on our recent result in [19], the present work aims to propose a robust digital-control scheme for continuous-time systems that can be used in two important scenarios: (i) having a high sampling frequency with limited computational power (ii) having a slow processor with jitter and irregular sampling times. Note that the second scenario occurs when the sampling frequency is relatively faster than the slow processing rate and, in addition, the sampling times are prone to delays and irregularities [20]. The main focus of this work will be on the first application (scenario), while the second application can be treated similarly.

In this paper, the sampled-data control of a continuous-time LTI system is studied, where the output of the system is sampled at a high rate. It is shown that every continuous-time stabilizing (LTI) controller can be implemented in a hybrid form consisting of a sampler, a digital processor, some so-called "modified second-order holds" and possibly a unity feedback from the holder to the sampler. This hybrid controller benefits from the fact that the increase of the sampling frequency has a direct influence only on the memory size of the controller, as opposed to its parameters. This property makes the parameters of the controller robust to the sampling rate. Moreover, it is proven that designing a continuous-time controller whose associated digital controller requires the least processing time amounts to a well-studied control problem.

The rest of the paper is organized as follows. Some preliminaries on conventional sampled-data control systems are provided in Section II and the problem is formulated accordingly. The main results are derived in Section III, which are illustrated with a numerical example in Section IV. Finally, some concluding remarks are given in Section V.

Notation: Throughout this paper, the letters t, κ, s, ω and z denote the continuous-time, discrete-time, Laplace-domain, Fourier-domain and Z-domain arguments, respectively. Moreover, time-domain signals are denoted by small letters, while their corresponding frequency/Laplace/Z-domain signals are represented by capitalized letters. For a continuous-time signal, say $h(t)$, the following notations are used:

- $h[\kappa]$: A discrete signal obtained from $h(t)$ by sampling.

The authors are with the Department of Control and Dynamical Systems, California Institute of Technology, Pasadena, USA (emails: lavaei@cds.caltech.edu; sojoudi@cds.caltech.edu; murray@cds.caltech.edu).

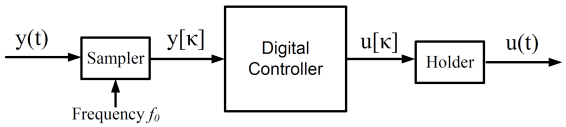

Fig. 1. This figure illustrates a conventional sampled-data control system.

- $H(s)$: Laplace transform of $h(t)$.
- $H(j\omega)$: Fourier transform of $h(t)$.
- $H[z]$: Z-transform of $h[\kappa]$.

II. Preliminaries and Problem Formulation

Consider a linear time-invariant (LTI) system $\mathcal{S}$ with the state-space representation

$$\begin{aligned} \dot{x}(t) &= Ax(t) + Bu(t), \\ y(t) &= Cx(t), \end{aligned} \tag{1}$$

where $x(t) \in \mathbf{R}^n$, $u(t) \in \mathbf{R}^m$ and $y(t) \in \mathbf{R}^r$ denote the state, input and output of the system, respectively. There are numerous applications for which it is required/preferable to control the system $\mathcal{S}$ using a digital controller, e.g. a micro-controller. A conventional digital-control scheme, referred to as *sampled-data control system*, is depicted in Figure 1, which consists of the following components:

- *Sampler:* This part is intended to sample the output of the system $\mathcal{S}$ at a pre-specified frequency f_0.
- *Digital Controller:* This controller processes the digital signal provided by the sampler.
- *Holder:* This part generates the input of the system $\mathcal{S}$ by converting the discrete-time output of the digital controller to a continuous-time signal.

Unlike an ideal sampler, there exist different types of ideal holders such as zero-order hold, first-order hold and second-order hold. Note that a zero-order hold has no memory for digital-to-analog conversion, while a first/second-order hold employs some integrators to generate an analog signal based on a history of the digital samples. After choosing a sampling frequency and a proper type of holder, the main challenge is to design a digital controller, denoted by G_d, for the sampled-data control system in such a way that the closed-loop system satisfies certain design specifications. To this end, three methods have been long studied in the literature:

i) Design a controller G_d for the discrete-time equivalent model of the system $\mathcal{S}$.
ii) Design G_d by first finding a continuous-time (finite-dimensional) controller G for the system $\mathcal{S}$ and then discretizing it.
iii) Design G_d directly for the time-varying closed-loop system.

(Instead of the step-invariant method, one can use other existing methods such as the Tustin approximation). With the ongoing technological advances, it is now possible to sample the outputs of many real-world systems at a very high rate f_0 in the order of several kilohertz. Although a high sampling rate is desirable for collecting more information from the continuous-time output $y(t)$, a sampled-data controller designed using the aforementioned techniques may suffer from some robustness issues for a relatively large f_0. To illustrate this fact, consider method (ii) and assume that the holder of the sampled-data control system is a zero-order hold. Let G be a given finite-dimensional, continuous-time controller designed for the system $\mathcal{S}$, with the state-space representation

$$\begin{aligned} \dot{x}_c(t) &= A_c x_c(t) + B_c y(t), \\ u(t) &= C_c x_c(t) + D_c y(t). \end{aligned} \tag{2}$$

The digital controller G_d can be taken as the discrete-time equivalent model of G obtained using the step-invariant method, which turns out to be

$$\begin{aligned} x_d[\kappa+1] &= A_d x_d[\kappa] + B_d y[\kappa], \\ u[\kappa] &= C_d x_d[\kappa] + D_d y[\kappa], \quad \kappa = 0, 1, 2, ..., \end{aligned} \tag{3}$$

where

$$\begin{aligned} &A_d = e^{hA_c}, \quad B_d = \int_0^h e^{tA_c} dt \; B_c, \\ &C_d = C_c, \quad D_d = D_c, \quad h = \frac{1}{f_0} \end{aligned} \tag{4}$$

(Instead of the step-invariant method, one can use other existing methods such as the Tustin approximation). observe that as the sampling period h goes to 0, A_d and B_d converge to I and 0, respectively. This implies that the convergence is independent of the values of the matrices A_c and B_c, which makes the digital controller G_d extremely fragile and sensitive to measurement and numerical round-off errors. By denoting the order of the controller G with n_c, it can be argued that this undesirable sensitivity is a consequence of generating the input $u[\kappa]$ in terms of the last n_c+1 samples of the output, i.e. $y[\kappa], y[\kappa-1], ..., y[\kappa-n_c]$. More precisely, as h goes to zero, all these samples become indistinguishable and, therefore, performing numerical computations on them leads to a poor strategy. This observation is valid for the aforementioned methods (i) and (iii) as well. A question arises as to whether it is possible to generate $u[\tau]$ in terms of some sufficiently distant samples, namely $y[\kappa-\tau_1], y[\kappa-\tau_2], ..., y[\kappa-\tau_p]$ for some disparate numbers $\tau_1, \tau_2, ..., \tau_p$, and deploy a new type of (fast) holder so that the resulting digital controller becomes satisfactorily robust and easily implementable (note that the idea of using distant output samples is not equivalent to slow sampling). This problem will be addressed here under the assumption that both sampler and holder operate at the same high frequency. The results can be easily generalized to the case when the holder (or actuator) operates at a slower frequency.

III. Control of Embedded Systems

The objective of this section is twofold. First, we show how a given continuous-time controller G can be implemented via a robust hybrid controller consisting of an ideal sampler with an arbitrarily high sampling frequency f_0, a digital processor and a modified second-order hold. Then, we investigate how the controller G can be designed in an optimal way so that its hybrid implementation is as simple as possible.

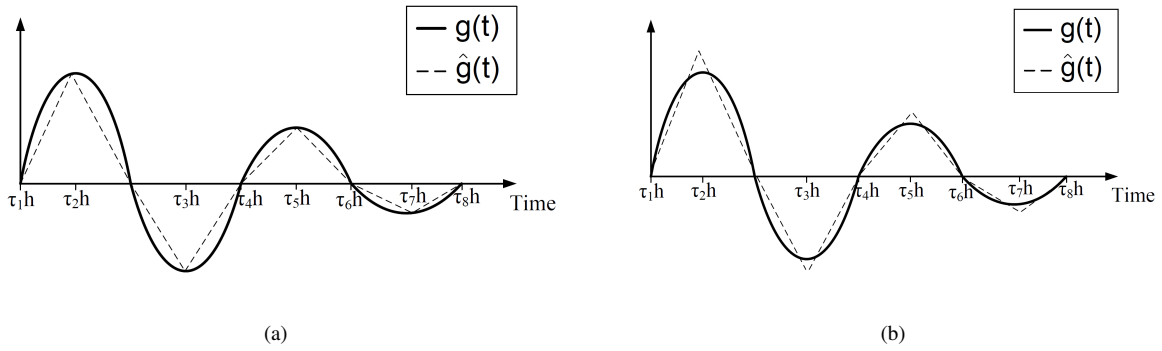

Fig. 2. These figures illustrate different piecewise linear approximations of an impulse response $g(t)$.

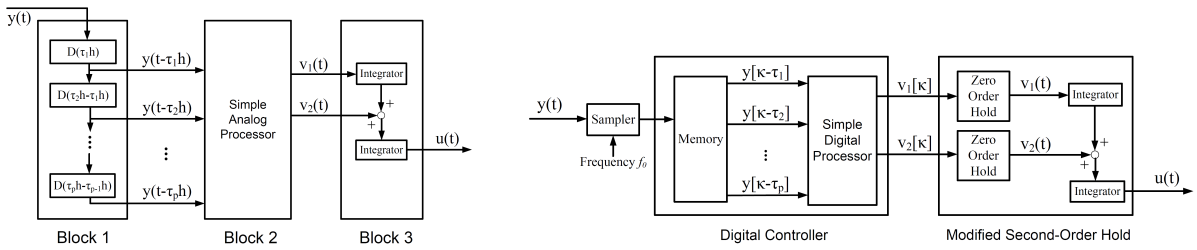

Fig. 3. (a) An analog implementation of the controller $\hat{G}(s)$; (b) The hybrid controller $\hat{G}_d$ associated with the continuous-time controller $\hat{G}$.

A. Digital Implementation with a High Sampling Rate

Given an LTI continuous-time controller G satisfying some prescribed design specifications, the goal is to implement this controller in the form of the configuration given in Figure 1 with a high sampling rate f_0. Assume for now that G is stable and single-input single-output. These assumptions will be removed later in this subsection. In addition, with no loss of generality, suppose that D_c is equal to 0 (because this term corresponds to a direct static feedback from $y(t)$ to $u(t)$ that can be easily implemented). Let $g(t)$ denote the impulse response of the controller G. The first step is to approximate the time-domain signal $g(t)$ by a piecewise linear signal with a finite number of breakpoints all belonging to the set $\{0, h, 2h, ...\}$. Denote this approximating signal as $\hat{g}(t)$. As an example, an exponentially decaying and oscillatory signal $g(t)$ is approximated by a function $\hat{g}(t)$ in Figure 2(a), which includes 8 breakpoints $\tau_1 h, \tau_2 h, ..., \tau_8 h$ for some integers $\tau_1, .., \tau_8$. It is worth mentioning that the approximating signal $\hat{g}(t)$ need neither be a continuous signal nor overlap with the original signal $g(t)$ at the breakpoints (corners), as demonstrated in Figure 2(b).

Denote the Laplace transforms of $g(t)$ and $\hat{g}(t)$ as $G(s)$ and $\hat{G}(s)$, respectively. It is straightforward to show that $\hat{G}(s)$ can be written as

$$\hat{G}(s) = \sum_{i=1}^{p} \left(\frac{\alpha_i}{s^2} + \frac{\beta_i}{s} \right) e^{-\tau_i h s}, \tag{5}$$

for some scalars $\alpha_1, ..., \alpha_p, \beta_1, ..., \beta_p$, where $\tau_1 h, ..., \tau_p h$ denote the breakpoints of the signal $\hat{g}(t)$ in an ascending order. There are two important properties regarding $\hat{G}(s)$ that have been studied in our recent paper [19]:

- Despite the fact that the controller $G(s)$ needs n_c integrators to be implemented, its approximating controller $\hat{G}(s)$ requires only two integrators and p delay blocks.
- The approximating signal $\hat{g}(t)$ can be contrived in such a way that the infinity norm of the error $G(s) - \hat{G}(s)$ becomes less than any prescribed tolerance.

Regarding the second point made above, it is shown in [19] that if $\hat{g}(t)$ overlaps with $g(t)$ at its breakpoints, then the approximation error $\|G(s) - \hat{G}(s)\|_\infty$ satisfies the following inequality:

$$\begin{aligned} \|G(s) - \hat{G}(s)\|_\infty \leq \sqrt{2} \int_0^{\tau_1 h} |g(t)| dt + \sqrt{2} \int_{\tau_p h}^{\infty} |g(t)| dt \\ + \sum_{i=1}^{p-1} \max_{t \in [\tau_i h, \tau_{i+1} h]} |g''(t)| \frac{\sqrt{2}(\tau_{i+1} h - \tau_i h)^3}{12}, \end{aligned} \tag{6}$$

where $g''(t)$ is the second derivative of $g(t)$ and $\|\cdot\|_\infty$ denotes the infinity norm. Given a prescribed maximum error, it is discussed in [19] how to find a permissible $\hat{g}(t)$ based on either $g(t)$ directly or its discretized counterpart with the discretization step h (the complexity of finding $\hat{g}(t)$ using the latter method is linear with respect to the number of discrete samples). An analog implementation of the controller $\hat{G}(s)$ is visualized in Figure 3(a), which consists of three blocks as follows:

- Block 1 delays the incoming signal $y(t)$ by $\tau_1 h, ..., \tau_p h$ seconds.

- Block 2 performs basic math operations to generate the signals $v_1(t) := \sum_{i=1}^{p} \alpha_i y(t-\tau_i h)$ and $v_2(t) := \sum_{i=1}^{p} \beta_i y(t-\tau_i h)$.
- Block 3 employs two integrators to generate $u(t)$ from $v_1(t)$ and $v_2(t)$.

Definition 1: Define $\hat{G}_d$ to be a hybrid controller with the configuration depicted in Figure 3(b), corresponding to the continuous-time controller $\hat{G}$.

Notice that $\hat{G}_d$ is obtained from the particular configuration of $\hat{G}$ given in Figure 3(a) using the following steps:

- Block 1 is replaced by an ideal sampler with the sampling frequency f_0.
- Block 2 is substituted by a memory capable of storing the last τ_p+1 samples of $y(t)$ and a simple digital processor for computing $v_1[\kappa] := \sum_{i=1}^{p} \alpha_i y[\kappa-\tau_i]$ and $v_2[\kappa] := \sum_{i=1}^{p} \beta_i y[\kappa-\tau_i]$.
- Block 3 is replaced by two zero-order holds and two integrators. This resulting block can be regarded as a "modified second-order hold" because of its analogy to a standard second-order hold that consists of a conventional digital-to-analog converter and two integrators (analog circuits).

The hybrid controller $\hat{G}_d$ introduced above is indeed a sampled-data controller with an ideal sampler and a modified second-order hold. Recall that the parameters A_d and B_d of a controller G_d obtained using a conventional discretization method converge to I and 0 as h tends to zero, which makes the controller sensitive to measurement and computational errors. In contrast, the correlation between the parameters $\alpha_1, ..., \alpha_p, \beta_1, ..., \beta_p$ of the controller $\hat{G}_d$ and the sampling period h is minimal in the sense that the precision of these parameters need not be increased as h goes to zero. Indeed, reducing h mainly affects the memory size, rather than the foregoing coefficients. This key property makes the hybrid controller $\hat{G}_d$ suitable for fast-sampling applications.

We wish to study the error resulting from implementing the continuous-time controller $\hat{G}$ as the hybrid controller $\hat{G}_d$. To this end, note that although $\hat{G}$ is time-invariant, its counterpart $\hat{G}_d$ is time-varying. In order to bypass the time-varying nature of this hybrid controller, since the system $\mathcal{S}$ acts as a low-pass filter (due to being strictly proper) and the sampling frequency f_0 is relatively high, it is reasonable to assume that high-frequency harmonics of the output signal $y(t)$ in the system $\mathcal{S}$ under $\hat{G}$ or $\hat{G}_d$ are negligible. Hence, assume that the output of the system $\mathcal{S}$ goes through an ideal low-pass filter $\mathcal{F}$ with the cut-off frequency $\omega_0 := \frac{2\pi}{h}$ before being processed by the controller. Let $\mathcal{F}\circ\hat{G}$ and $\mathcal{F}\circ\hat{G}_d$ denote the cascades of the filter $\mathcal{F}$ with the controllers $\hat{G}$ and $\hat{G}_d$, respectively.

Theorem 1: The hybrid controller $\mathcal{F}\circ\hat{G}_d$ is linear time-invariant with the transfer function

$$\mathcal{F}\circ\hat{G}_d(j\omega) = \begin{cases} \mathcal{F}\circ\hat{G}(j\omega)\cdot\left(e^{-j\omega\frac{h}{2}}\frac{\sin\left(\omega\frac{h}{2}\right)}{\omega\frac{h}{2}}\right) & \omega\in[-\omega_0,\omega_0] \\ \mathcal{F}\circ\hat{G}(j\omega) & \text{otherwise} \end{cases} \tag{7}$$

Proof: In the cascade controller $\mathcal{F}\circ\hat{G}_d$, let $y_f(t)$, $y(t)$ and $u(t)$ denote the incoming signal of $\mathcal{F}$, the incoming signal of $\hat{G}_d$ and the output of $\hat{G}_d$, respectively. Due to the presence of the filter $\mathcal{F}$, the relation $\mathcal{F}\circ\hat{G}_d(j\omega) = \mathcal{F}\circ\hat{G}(j\omega) = 0$ holds if $\omega \notin [-\omega_0,\omega_0]$. Now, consider a frequency $\omega\in[-\omega_0,\omega_0]$. It can be verified that (see [4], Chapter 3)

$$\begin{aligned} Y\left[e^{-j\omega h}\right] &= \frac{1}{h}\left(\sum_{k=-\infty}^{\infty} Y(j\omega+jk\omega_0)\right) = \frac{1}{h}Y_f(j\omega), \\ V_1[z] &= \left(\sum_{i=1}^{p}\alpha_i z^{-\tau_i}\right)Y[z], \\ V_1(j\omega) &= h\left(e^{-j\omega\frac{h}{2}}\frac{\sin\left(\omega\frac{h}{2}\right)}{\omega\frac{h}{2}}\right)V_1\left[e^{-j\omega h}\right]. \end{aligned} \tag{8}$$

Thus,

$$V_1(j\omega) = \left(e^{-j\omega\frac{h}{2}}\frac{\sin\left(\omega\frac{h}{2}\right)}{\omega\frac{h}{2}}\right)\left(\sum_{i=1}^{p}\alpha_i e^{-j\omega h\tau_i}\right)Y_f(j\omega). \tag{9}$$

Similarly,

$$V_2(j\omega) = \left(e^{-j\omega\frac{h}{2}}\frac{\sin\left(\omega\frac{h}{2}\right)}{\omega\frac{h}{2}}\right)\left(\sum_{i=1}^{p}\beta_i e^{-j\omega h\tau_i}\right)Y_f(j\omega). \tag{10}$$

The proof follows immediately from the equations (9) and (10). ■

Recall that the approximating controller $\hat{G}$ can be arbitrarily close to the original controller G. On the other hand, Theorem 1 states that the hybrid controller $\hat{G}_d$ behaves differently from its continuous-time counterpart $\hat{G}$ by a factor $e^{-j\omega\frac{h}{2}}\frac{\sin\omega\frac{h}{2}}{\omega\frac{h}{2}}$ in the Fourier domain if its incoming signal has no harmonics at frequencies greater than ω_0. Notice that as h goes to 0, the real-valued factor $\frac{\sin\omega\frac{h}{2}}{\omega\frac{h}{2}}$ tends to 1 and so does the complex-valued factor $e^{-j\omega\frac{h}{2}}$. As a result, $\hat{G}_d$ is a digital implementation of the original controller G. In order to mitigate the effect of the discretization error $e^{-j\omega\frac{h}{2}}\frac{\sin\omega\frac{h}{2}}{\omega\frac{h}{2}}$, it is desired to manipulate the controller $\hat{G}_d$ such that its discrepancy with the original controller $\hat{G}$ becomes only a multiplicative real-valued factor $\frac{\sin\omega\frac{h}{2}}{\omega\frac{h}{2}}$. To this end, the following procedure can be taken.

Procedure 1:

- Approximate $g(t)$ with a piecewise linear function $\tilde{g}_d(t)$ in such a way that its breakpoints lie in the set $\{\frac{h}{2}, \frac{3h}{2}, \frac{5h}{2}, ...\}$, as opposed to $\{0, h, 2h, ...\}$.
- Find the Laplace transform of $\tilde{g}_d(t)$ and write it in the form of

$$\sum_{i=1}^{p}\left(\frac{\alpha_i}{s^2}+\frac{\beta_i}{s}\right)e^{-(\tau_i h+\frac{h}{2})s}. \tag{11}$$

- Define $\tilde{G}_d$ to be the hybrid controller depicted in Figure 3(b), where

$$v_1[\kappa] := \sum_{i=1}^{p}\alpha_i y[\kappa-\tau_i], \quad v_2[\kappa] := \sum_{i=1}^{p}\beta_i y[\kappa-\tau_i]. \tag{12}$$

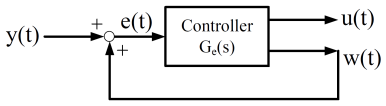

Fig. 4. An equivalent implementation of an unstable controller $G(s)$.

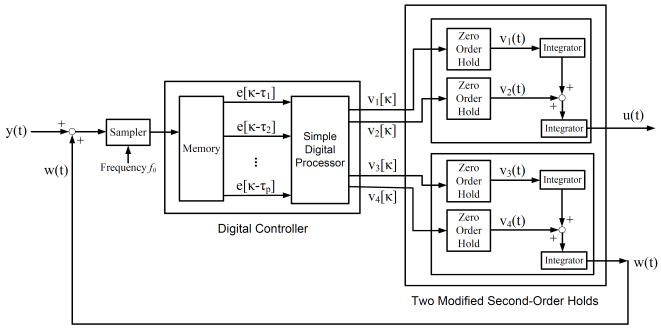

Fig. 5. The hybrid controller $\hat{G}_d$ associated with an unstable continuous-time controller G.

- The system $\mathcal{F} \circ \tilde{G}_d$ is LTI with the transfer function

$$\mathcal{F}\circ\tilde{G}_d(j\omega) = \begin{cases} \mathcal{F} \circ \tilde{G}(j\omega) \cdot \left(\frac{\sin(\omega \frac{h}{2})}{\omega \frac{h}{2}} \right) & \omega \in [-\omega_0, \omega_0] \\ \mathcal{F} \circ \tilde{G}(j\omega) & \text{otherwise} \end{cases} \tag{13}$$

The hybrid controller $\tilde{G}_d$ introduced in Procedure 1 is another digital implementation of G which, in comparison to the hybrid controller $\hat{G}_d$, is expected to have less discrepancy with respect to the target controller $\hat{G}$.

Th results developed so far are based on the assumption that the initial controller $G(s)$ is stable. Now, suppose that this stabilizing controller is not stable itself. Since G stabilizes the system $\mathcal{S}$, the pair (A_c, B_c) is stabilizable. Therefore, there exists a matrix gain $L \in \mathbf{R}^{1\times n_c}$ such that $A_c - B_c L$ is Hurwitz. Define $w(t) := Lx_c(t)$ and $e(t) := y(t) + w(t)$. The controller G is equivalent to the feedback configuration given in Figure 4, whose backward path is a unity feedback and whose forward path is a controller $G_e(s)$ with the control law

$$\begin{aligned} \dot{x}_c(t) &= (A_c - B_c L)x_c(t) + B_c e(t), \\ u(t) &= C_c x_c(t), \\ w(t) &= Lx_c(t). \end{aligned} \tag{14}$$

It can be observed that the controller $G_e(s)$ with the single input $e(t)$ and the outputs $u(t)$ and $w(t)$ is stable. Now, each of the transfer functions from "$e(t)$ to $u(t)$" and "$e(t)$ to $w(t)$" can be implemented via its hybrid counterpart explained earlier. Hence, the unstable controller $G(s)$ can be implemented in the sampled-data control scheme depicted in Figure 5, which consists of an ideal sampler, a digital controller, two modified second-order holds and a unity feedback. Note that it may not be possible in practice to add the signals $y(t)$ and $w(t)$ before sampling, as suggested in Figure 5. As an alternative, the output of the system, i.e. $y(t)$, can be sampled individually and then be added to the samples of the signal $w(t)$ which is already available in the output of the hybrid controller.

Remark 1: Assume that the controller $G(s)$ is multi-input single-output. The results developed earlier can be adopted to show that:

- If $G(s)$ is stable, it can be implemented in the hybrid form given in Figure 3(b).
- If $G(s)$ is unstable, it can be implemented in the hybrid form depicted in Figure 5 with the difference that its holder might need more than two modified second-order holds. In fact, although the scalar $u(t)$ needs only one modified second-order hold, the vector signal $w(t)$ requires as many modified second-order holds as the number of nonzero rows of the auxiliary matrix L. Note that if, for instance, $G(s)$ is stabilizable through one of its single inputs, there exists a proper matrix L with only one nonzero row.

In the case when $G(s)$ is a multi-input multi-output controller, regard this as a set of multi-input single-output sub-controllers and then apply the above result to each of these sub-controllers. Hence, each of the single outputs of $G(s)$ that is to be applied to the system $\mathcal{S}$ needs one or more modified second-order holds for actuation.

Remark 2: The hybrid controllers $\hat{G}_d$ and $\tilde{G}_d$ proposed in this paper are designed based on a piecewise linear approximation of the impulse response of the original controller G. It might be speculated that a hybrid controller with the configuration given in Figure 3(b) can be designed directly, possibly by using the lifting technique [4]. Nonetheless, it is to be noted that since the unknown discrete delays $\tau_1, \tau_2, ..., \tau_p$ could be several times larger than the order of the original controller G, designing $\hat{G}_d$ directly is formidable.

B. Near-Optimal Hybrid Controller Design

Assume that the system $\mathcal{S}$ is strongly stabilizable, meaning that there exists a stable stabilizing controller $G(s)$ for this system. Note that the strong stabilization of $\mathcal{S}$ can be easily verified using a well-known pole-zero test [23]. Suggested by the discussion made earlier, assume with no loss of generality that $G(s)$ is multi-input single-output. It was demonstrated in the preceding subsection that $G(s)$ can be implemented in the hybrid configuration depicted in Figure 3(b). The main complexity of this digital-control scheme (the required processing time) is contingent upon the number of delays $\tau_1, \tau_2, ..., \tau_p$. Given some design specifications, since there are often an infinite number of stable controllers $G(s)$ satisfying these specifications, the objective of this subsection is to find the one whose digital implementation using the method developed here requires the least number of delays. To this end, depending on whether or not the order of the controller $G(s)$ being sought is fixed *a priori*, two methods will be proposed in the sequel. Note that the results developed next can be extended to the case when the hybrid configuration in Figure 5 must be employed due to the non-existence of a stable stabilizing controller $G(s)$.

For the first method, we design a controller $G(s)$ with a near-optimal digital implementation and of a pre-specified degree n_c for which certain design specifications, denoted by $\mathcal{D}$, are satisfied. Assume that the control specifications $\mathcal{D}$ can be translated into a matrix inequality as

$$\mathcal{L}(A_c, B_c, C_c, R) \prec 0, \tag{15}$$

for some bilinear matrix operator $\mathcal{L}$ and a slack (matrix) variable R, where $\prec$ represents the matrix inequality in the negative-definite sense. It is noteworthy that many specifications such as guaranteed H_2 performance, guaranteed H_∞ performance, robust pole-placement or any combinations of these specifications can be expressed in the above form (even the ones involving rank constraints) [21], [22]. In the case when h is relatively small, the simplicity of the best piecewise linear approximation of $g(t)$ with the breakpoints belonging to $\{0, h, 2h, ...\}$ is directly related to how smooth this function is. Hence, the performance index

$$J := \int_0^\infty \|g''(t)\|_2^2 \ dt, \tag{16}$$

where $\|\cdot\|_2$ denotes the 2-norm operator, is a measure of how hard $g(t)$ can be approximated by a piecewise linear function. In particular, when J is equal to 0, the impulse response $g(t)$ must be a line. Thus, the goal is to minimize the performance index J in order to find a controller $G(s)$ whose digital implementation is near-optimal. The stabilizable controller $G(s)$ being found can be assumed to be both controllable and observable (because an infinitesimal perturbation of a stabilizable controller always makes it controllable and observable). The state-space representation (A_c, B_c, C_c) of $G(s)$ can be considered to be in the observable form, implying that C_c is equal to $\begin{bmatrix} 1 & 0 & \cdots & 0 \end{bmatrix}$. Therefore, the only unknown parameters are A_c and B_c. We introduce the following optimization problem.

Optimization 1: Minimize the scalar α subject to

$$\mathcal{L}(A_c, B_c, C_c, R) \prec 0, \tag{17a}$$

$$\begin{bmatrix} A_cP + PA_c^T & A_cB_c \\ B_c^TA_c^T & -I \end{bmatrix} \prec 0, \tag{17b}$$

$$\begin{bmatrix} -\alpha & C_cA_cP \\ PA_c^TC_c^T & -P \end{bmatrix} \prec 0, \tag{17c}$$

for matrix variables $A_c \in \mathbf{R}^{n_c \times n_c}$ and $B_c \in \mathbf{R}^{n_c \times r}$, a symmetric matrix variable $P \in \mathbf{R}^{n_c \times n_c}$ and a slack variable R of appropriate dimension, where A_c is in the (observable) canonical form.

Denote the optimal values of the matrices A_c and B_c solving Optimization 1 with A_c^* and B_c^*, respectively.

Theorem 2: The controller $G(s)$ with the state-space matrices (A_c^*, B_c^*, C_c) is stable, satisfies the design specifications $\mathcal{D}$ and minimizes the performance index J.

Proof: Given a controllable, observable, and stable controller $G(s)$ with the matrices (A_c, B_c, C_c), one can write

$$g(t) = C_ce^{A_ct}B_c, \quad \forall t \geq 0. \tag{18}$$

Hence,

$$g''(t) = C_cA_ce^{A_ct}A_cB_c, \quad \forall t \geq 0. \tag{19}$$

As a result, the performance index J can be obtained as

$$J = \int_0^\infty C_cA_ce^{A_ct}A_cB_cB_c^TA_c^Te^{A_c^Tt}A_c^TC_c^T dt, \tag{20}$$

or equivalently $J = C_cA_cPA_c^TC_c^T$, where P is the unique solution of the Lyapunov equation

$$A_cP + PA_c^T + A_cB_cB_c^TA_c^T = 0. \tag{21}$$

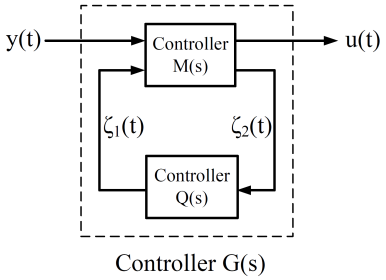

Fig. 6. A generic model for the stabilizing controller $G(s)$.

Now, it can be proved that J is equal to the minimum (infimum) of a scalar α subject to the constraints

$$A_cP + PA_c^T + A_cB_cB_c^TA_c^T \prec 0, \tag{22a}$$

$$C_cA_cPA_c^TC_c^T \prec \alpha, \tag{22b}$$

$$-P \prec 0. \tag{22c}$$

The Schur complement formula can be used twice to deduce that the above constraints are identical to (17b) and (17c). ■

Theorem 2 states that Optimization 1 yields a controller $G(s)$ whose digital implementation is near-optimal. Nevertheless, regardless of the constraint (17a) corresponding to the given design specifications, the other constraints in Optimization 1 are nonlinear with respect to the variables A_c, B_c and P. This is a common issue in many control problems for designing a fixed-order controller [22]. However, it can be observed that if either A_c or B_c, P are fixed, the constraints (17b) and (17c) turn into linear matrix inequalities. Hence, one can start from a stable controller and solve this optimization problem iteratively by fixing A_c and B_c, P alternatively until a local solution is found (see [16] and the references therein for similar algorithms).

So far, it was assumed that the design specification $\mathcal{D}$ is rather general. Now, suppose that the only specification is the stability of the closed-loop system, and that the order of the controller being found is not set *a priori*. As the second method, the goal is to study how this special problem is related to the existing well-studied problems in the literature. To this end, first remove the assumption that $G(s)$ is strictly proper and allow this controller to be biproper if necessary. Furthermore, let a variant of the performance index J be used for this method as follows. Consider a single-input single output, stable, low-pass filter $\bar{\mathcal{F}}(s)$ whose relative degree is greater than 2. Denote the impulse response of $\bar{\mathcal{F}}(s)G(s)$ with $\bar{g}(t)$. Define a new performance index $\bar{J}$ as

$$\bar{J} := \int_0^\infty \|\bar{g}''(t)\|_2^2 \ dt. \tag{23}$$

Note that unlike the performance index J, the new index $\bar{J}$ operates on the filtered impulse response to remove any possible jitter that makes the second derivative of $g(t)$ unnecessarily high but does not affect the piecewise linear approximation of $g(t)$ noticeably. It will be shown in the sequel that although finding a stable, stabilizing controller $G(s)$ minimizing $\bar{J}$ may not be a convex problem, it can be cast as a well-known problem for which there exist different sufficient conditions in the convex form.

Since $\bar{\mathcal{F}}(s)$ is stable with a relative degree greater than 2, the transfer function $s^2\bar{\mathcal{F}}(s)$ has a state-space realization as $(A_f, B_f, C_f, 0)$, where A_f is a Hurwitz matrix. Design two matrix gains $L_1 \in \mathbf{R}^{m\times n}$ and $L_2 \in \mathbf{R}^{n\times r}$ such that the matrices $A + BL_1$ and $A + L_2C$ become both Hurwitz. Consider the system

$$\begin{aligned}\dot{\mathbf{x}}_f(t) =& \begin{bmatrix} A+BL_1+L_2C & 0 \\ B_fL_1 & A_f \end{bmatrix}\mathbf{x}_f(t) \\ &+ \begin{bmatrix} -L_2 \\ 0 \end{bmatrix} y(t) + \begin{bmatrix} B \\ B_f \end{bmatrix}\zeta_1(t), \qquad (24a)\\ u_f(t) =& \begin{bmatrix} 0 & C_f \end{bmatrix}\mathbf{x}_f(t), \qquad (24b)\\ \zeta_2(t) =& \begin{bmatrix} -C_2 & 0 \end{bmatrix}\mathbf{x}_f(t) + y(t), \qquad (24c)\end{aligned}$$

with the inputs $y(t), \zeta_1(t)$ and the outputs $u_f(t), \zeta_2(t)$. Find a finite-dimensional, stable, LTI controller from $\zeta_2(t)$ to $\zeta_1(t)$ to minimize the 2-norm of the transfer function from $y(t)$ to $u_f(t)$ in above control system, and denote it with $Q^*(s)$. It can be observed that finding $Q^*(s)$ amounts to a standard H_2 *strong stabilization* problem. Note that the closely related problems of H_2 *strong stabilization* and H_∞ *strong stabilization* have been thoroughly investigated in several works [23], [24], [25], [26].

Theorem 3: Let $G(s)$ be taken as the controller given in Figure 6 with $Q(s)$ equal to $Q^*(s)$ and $M(s)$ with the control law

$$\begin{aligned}\dot{\mathbf{x}}(t) &= (A + BL_1 + L_2C)\mathbf{x}(t) - L_2y(t) + B\zeta_1(t),\\ u(t) &= L_1\mathbf{x}(t) + \zeta_1(t),\\ \zeta_2(t) &= -C\mathbf{x}(t) + y(t).\end{aligned} \qquad (25)$$

This choice of the controller $G(s)$ is stable, stabilizes the system $\mathcal{S}$ and minimizes the performance index $\bar{J}$.

Sketch of Proof: It follows from the linear fractional transformation that every stabilizing, finite-dimensional, LTI controller $G(s)$ can be decomposed into the form given in Figure 6 for some stable controller $Q(s)$ [4]. Augment the controller $G(s)$ with the modified filter $s^2\bar{\mathcal{F}}(s)$ by connecting the filter to the output of the controller $G(s)$, and denote the output of the augmented system with $u_f(t)$. It can be observed that the impulse response of the augmented system is equal to $\bar{g}''(t)$. This result is due to the facts that $s^2\bar{\mathcal{F}}(s)$ is strictly proper and that the term s^2 acts as a double differentiator. Now, it can be concluded from Parseval's theorem that $\int_0^\infty \|\bar{g}''(t)\|_2^2\ dt$ is equal to the 2-norm of the transfer function of the augmented system from $y(t)$ to $u_f(t)$. The proof is completed by noting that the model (24) under the controller $Q(s)$ from $\zeta_2(t)$ to $\zeta_1(t)$ is a state-space representation of this augmented system. ■

Theorem 3 states that finding a stable, stabilizing controller $G(s)$ with a near-optimal digital implementation amounts to the well-studied problem of *stable H_2 optimal control* (or H_2 *strong stabilization*). Note that the filter $\bar{\mathcal{F}}(s)$ should be chosen meticulously in order to have a useful index $\bar{J}$ that truly accounts for the smoothness of $g(t)$. As an alternative to the index $\bar{J}$, it can be shown that the minimization of the simple index $\int_0^\infty \|g(t)\|_2^2\ dt$ (with no differentiation involved) also leads to a near-optimal $g(t)$. This minimization can be converted to finding a stable H_2 optimal controller $Q(s)$ for the configuration given in Figure 6.

Two indices J and $\bar{J}$ were introduced in this subsection to design a controller $G(s)$ with a smooth impulse response. Once the function $g(t)$ is obtained using either of the above-mentioned methods, the technique outlined in [19] can be used to find a minimal set of delays $\{\tau_1, \tau_2, ..., \tau_p\}$.

IV. Numerical Example

Consider the 8th order unstable system given in Section VI of our recent paper [19], for which an optimal LQG controller $G(s) = \frac{G_1(s)}{G_2(s)}$ was designed (with respect to the weighting matrices $Q = I$, $R = 1$ and the identity noise covariance), where

$$\begin{aligned}G_1(s) :=& 15.76s^7 - 3.896s^6 + 60.68s^5 - 9.68s^4 \\ &+ 34.99s^3 - 2.064s^2 - 12.39s + 0.2986,\\ G_2(s) :=& s^8 + 8.684s^7 + 41.18s^6 + 115.3s^5 + 208.8s^4 \\ &+ 250.9s^3 + 197.9s^2 + 111.1s + 26.64.\end{aligned} \qquad (26)$$

Let the initial state of the system be the vector $[1\ 1\ \cdots\ 1]$. The objective of this section is to implement this controller in a sampled-data control configuration with the sampling frequency $f_0 = 100$Hz under the assumption that the precision of the parameters of the digital controller is confined to four fractional digits. This assumption is made to ensure that the digital processor performs a reasonable truncation before any computation. As the first approach, let the controller $G(s)$ be converted to a conventional sampled-data controller using the step-invariant method and then the parameters of the digital controller be truncated to 4 significant fractional digits. The output of the system is plotted in Figure 7(a) to demonstrate that the closed-loop system is unstable. Note that this instability is only the result of reducing the infinite precision to four digits. If the sampling frequency is reduced to 10Hz, the closed-loop system will be still unstable, as illustrated in Figure 7(b).

In contrast, the controller $G(s)$ can be implemented in the hybrid configuration $\hat{G}_d$ with the parameters

$$\begin{aligned}&\begin{bmatrix} \tau_1 & \tau_2 & \cdots & \tau_{12} \end{bmatrix} = \begin{bmatrix} 0 & 0.2 & 0.37 & 1.03 & 2 \\ & 3.15 & 4.7 & 6.7 & 10.1 & 13.55 & 17.11 & 20 \end{bmatrix},\\ &\begin{bmatrix} \alpha_1 & \alpha_2 & \cdots & \alpha_{12} \end{bmatrix} = \begin{bmatrix} -84.1100 & 68.3058 \\ 0.4660 & -0.1936 & 28.2217 & -16.3791 & 5.3132 \\ -1.6841 & 0.0895 & -0.0436 & 0.0223 & -0.0081 \end{bmatrix},\\ &\begin{bmatrix} \beta_1 & \beta_2 & \cdots & \beta_{12} \end{bmatrix} = \begin{bmatrix} 13.9861 & 0 & 0 & 0 \\ 0 & 0 & 0 & 0 & 0 & 0 & 0 & -0.0061 \end{bmatrix},\end{aligned} \qquad (27)$$

which are obtained using the approximation technique discussed in [19] and the method proposed here. The output and input of the system are plotted under both the continuous-time controller $G(s)$ and its hybrid implementation $\hat{G}_d$ in Figures 7(c) and 7(d). These figures clearly demonstrate that the proposed hybrid controller performs very similarly to the original LQG controller and that the high sampling frequency $f_0 = 100$Hz does not cause a robustness issue.

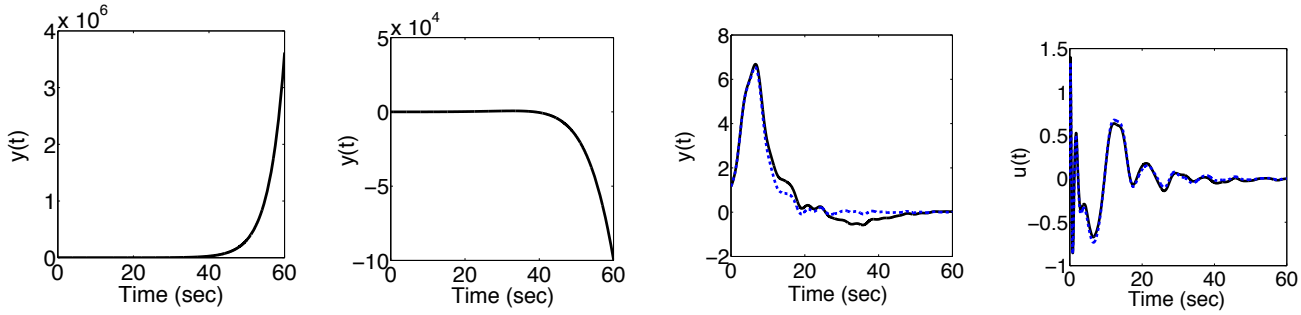

(a) (b) (c) (d)

Fig. 7. (a): The output of the system $\mathcal{S}$ under a conventional sampled-data controller with $f_0 = 100$Hz; (b): The output of the system $\mathcal{S}$ under a conventional sampled-data controller with $f_0 = 10$Hz; (c): The output of the system $\mathcal{S}$ under $G(s)$ (dotted curve) and $\hat{G}_d$ with $f_0 = 100$Hz (solid curve); (d): The input of the system $\mathcal{S}$ under $G(s)$ (dotted curve) and $\hat{G}_d$ with $f_0 = 100$Hz (solid curve).

V. Conclusions

Since a conventional sampled-data controller with a relatively high sampling frequency needs high-precision computation to cope with the robustness issues, this work proposes a new type of digital-control scheme for continuous-time systems associated with a high sampling frequency and low computational power. It is shown that every continuous-time stabilizing (LTI) controller can be implemented in a hybrid configuration composed of an ideal sampler, a digital controller, a number of modified second-order holds and possibly a unity feedback. The main advantage of this hybrid controller is that increasing the sampling frequency mainly affects the memory size of the controller, as opposed to its parameters. This property makes the controller robust to measurement and computational errors at high frequencies, and hence obviates the necessity of increasing the processing precision. Finding a continuous-time controller satisfying certain design specifications with a near-optimal digital implementation is also studied.

References

[1] K. J. Åström and B. Wittenmark, "Computer controlled systems: theory and design," *Prentice-Hall*, Englewood Cliffs, 1997.

[2] H. Kopetz, "Real-time systems: design principles for distributed embedded applications," *Norwell*, MA: Kluwer, 1997.

[3] E. I. Jury, "Sampled-data control systems," *Krieger Publishing Co.*, 1977.

[4] T. Chen and B. A. Francis, "Optimal sampled-data control systems," *Springer*, 1995.

[5] V. Zakian, "Control systems design: a new framework," Springer, 2005.

[6] B. Bamieh, J. Pearson, B. Francis, and A. Tannenbaum, "A lifting technique for linear periodic systems," *Systems & Control Letters*, vol. 17, no. 2, pp. 79-88, 1991.

[7] T. Hagiwara and M. Araki, "FR-operator approach to the H_2 analysis and synthesis of sampled-data systems," *IEEE Transactions on Automatic Control*, vol. 40, no. 8, pp. 1411-1421, 1995.

[8] J. Chen, S. Hara, L. Qiu, and R. Middleton, "Best achievable tracking performance in sampled-data systems via LTI controllers," *IEEE Transactions on Automatic Control*, vol. 53, no. 11, pp. 2467-2479, 2008.

[9] H. Fujioka, "Stability analysis for a class of networked/embedded control systems: A discrete-time approach," in *Proceedings of 2008 American Control Conference*, pp. 4997-5002, 2008.

[10] N. van de Wouw, P. Naghshtabrizi, M. Cloosterman, and J. Hespanha. "Tracking control for sampled-data systems with uncertain time-varying sampling intervals and delays," *International Journal of Robust and Nonlinear Control*, vol. 20, no. 4, pp. 387-411, 2009.

[11] G. M. Kranc, "Input-output analysis of multirate feedback systems," *IRE Transactions on Automatic Control*, vol. 3, pp. 21-28, 1957.

[12] S. Lall and G. Dullerud, "An LMI solution to the robust synthesis problem for multi-rate sampled-data systems," *Automatica*, vol. 37, no. 12, pp. 1909-1922, 2001.

[13] A. Feuer and G. C. Goodwin, "Generalized sample hold functions-frequency domain analysis of robustness, sensitivity, and intersample difficulties," *IEEE Trans. on Automat. Contrl.*, vol. 39, no. 5, pp. 1042-1047, 1994.

[14] J. Lavaei and A. G. Aghdam, "Pole assignment with improved control performance by means of periodic feedback," *IEEE Transactions on Automatic Control*, vol. 55, no. 1, pp. 248-252, 2010.

[15] P. T. Kabamba, "Control of linear systems using generalized sampled-data hold functions," *IEEE Trans. on Automat. Contrl.*, vol. 32, no. 9, pp. 772-783, 1987.

[16] J. Lavaei and A. G. Aghdam, "Simultaneous LQ control of a set of LTI systems using constrained generalized sampled-data hold functions," *Automatica*, vol. 43, no. 2, pp. 274-280, 2007.

[17] J. Lavaei and A. G. Aghdam, "Elimination of fixed modes by means of high-performance constrained periodic control," in *Proc. 45th IEEE Conf. on Decision and Contrl.*, San Diego, CA, pp. 4441-4447, 2006.

[18] A. Babakhani, X. Guan, A. Komijani, A. Natarajan, and A. Hajimiri, "A77-GHz phased array transceiver with on-chip antennas in silicon: receiver and antennas," *IEEE Journal of Solid-State Circuits*, vol. 41, no. 12, pp. 2795-806, 2006.

[19] J. Lavaei, S. Sojoudi, and R. M. Murray, "Simple delay-based controller design," to appear in *Proceedings of 2010 American Control Conference*, Baltimore, 2010 (available online at www.cds.caltech.edu/∼lavaei/ACC2010_Delay.pdf).

[20] M. Lluesma, A. Cervin, P. Balbastre, I. Ripoll, and A. Crespo, "Jitter evaluation of real-time control systems," in *12th IEEE International Conference on Embedded and Real-Time Computing Systems and Applications*, Sydney, 2006.

[21] S. Boyd, L. E. Ghaoui, E. Feron, and V. Balakrishnan, "Linear matrix inequalities in system and control theory," *SIAM*, 1994.

[22] G. E. Dullerud and F. Paganini, "A course in robust control theory: a convex approach," *Texts in Applied Mathematics, Springer*, 2005.

[23] C. Ganesh and J. B. Pearson, "H_2-optimization with stable controllers," *Automatica*, vol. 25, no. 4, pp. 629-634, 1989.

[24] C. Ganesh and J. B. Pearson, "A parametric optimization approach to H_∞ and H_2 strong stabilization," *Automatica*, vol. 39, no. 7, pp. 1205-1211, 2003.

[25] D. U. Campos-Delgado and K. Zhou, "H_∞ strong stabilization," *IEEE Transactions on Automatic Control*, vol. 46, no. 12, pp. 1968-1972 , 2001.

[26] S. Gumussoy and H. Ozbay, "Remarks on strong stabilization and stable H_∞ controller design," *IEEE Transactions on Automatic Control*, vol. 50, no. 12, pp. 2083-2087 , 2005.